ELSEVIER

Physica B 221 (1996) 267-283

PHYSICA B

On the reflectivity of polymers: Neutrons and X-rays

T.P. Russell

IBM Research Division, Almaden Research Center, 650 Harry Road, K131802, San Jose, CA 95120-6099, USA

Abstract

Over the last few years reflectivity methods have emerged as key tools for the investigation of polymer surfaces and interfaces. The high spatial resolution of these techniques, of the order of 5 Å, has provided a means of probing density gradients in polymers on a submolecular level. This resolution, coupled with selective labeling of all or parts of polymer chains has permitted the examination of polymers at surface and interfaces with unsurpassed detail. Herein, a brief review is given on the basic principles of reflectivity, a discussion of some of the areas where reflectivity has made an impact in polymers and a review of a systematic series of studies on block copolymers which serve as an ideal example to emphasize the strengths of reflectivity and how reflectivity can be used to extract detailed information on a specific problem.

1. Introduction

Over the past few years neutron and X-ray reflectivity have emerged as powerful tools for the investigation of the interfacial behavior of polymers. As testament to this, over the past eight years the number of publications per year where neutron reflectivity has been used has increased by an order of magnitude. In the case of X-rays, this number has quadrupled. Neither technique is new. X-ray reflectivity has been used for quite some time to investigate the surface roughness of materials and neutron reflectivity was used, initially, to determine the scattering length density of materials by the location of the critical angle. However, nearly a decade had past since the pioneering studies of Hayter and coworkers [1–3] using neutron reflectivity and Segmüller and coworkers [4, 5] using X-ray reflectivity to investigate the structure of Langmuir-Blodgett films in the early eighties before the true power of these techniques for the investigation of polymeric materials was realized. This delay, particularly in the case of neutrons, can be attributed to two principal factors. The first is the availability of sources and instrumentation where such measurements could be made. The second was the realization that polymeric films could be prepared smooth enough to utilize the high spatial resolution of the techniques. However, once these barriers were overcome, the use of these techniques has expanded enormously. In the United States alone there are currently nine neutron reflectometers available with several more under construction. In the case of X-rays, standard sealed sources can be used to this end, so that the number of X-ray reflectometers is, more than likely, in the hundreds. Since this surge in the use of reflectivity techniques, several comprehensive reviews have appeared on the subject [6–10].

This article is not meant to be a comprehensive review on the use of X-ray and neutron reflectivity for the investigation of polymers. Rather, some of the basic principles of reflectivity will be discussed, emphasizing some of the advantages and disadvantages of X-rays and neutrons. A brief overview of some of the areas in polymer science where reflectivity has been used decisively will be given . Then, one area in polymers will be discussed in detail where the power of X-ray and neutron reflectivity has been brought to bear. In particular, the behavior of thin films of diblock copolymers will be discussed where a series of studies have been undertaken to elucidate the morphology, ordering and transition behavior of these molecules in the vicinity of a surface. These studies serve as excellent examples showing the detail that one can extract from reflectivity, as well as, its limitations.

0921-4526/96/$15.00 © 1996 Elsevier Science B.V. All rights reserved
SSDI 0921-4526(95)00937-X

2. Reflectivity

In any scattering or reflectivity measurement it is necessary to have contrast between the species of interest and the surrounding medium. One can think of this as a variation in the refractive index n, where, for X-rays and neutrons, we can [11] write

$$n = 1 - \delta + i\beta, \tag{1}$$

where δ is the real part of the refractive index and β is the imaginary component which accounts for absorption. In the case of X-rays,

$$\delta_X = \lambda^2 \rho_{el} r_0 / 2\pi \tag{2}$$

and

$$\beta_X = \mu\lambda/4\pi, \tag{3}$$

where λ is the X-ray wavelength, ρ_{el} the electron density, r_0 the classical electron radius (2.82×10^{-13} cm) and μ the linear absorption coefficient. In the case of neutrons, for nonmagnetic materials, $\beta_N = 0$ and

$$\delta_N = \frac{N_A \rho \lambda^2}{2\pi} \frac{b_{mon}}{M_{mon}}, \tag{4}$$

where ρ is the mass density and M_{mon} the molecular weight of a monomer unit having a scattering length of b_{mon}, which is a sum over all nuclei in the monomer. One point needs to be made concerning the β for both X-rays and neutrons. The absorption depends, in the case of X-rays, on the interaction of the incident photons with the electrons in the sample, whereas for neutron, it is the interaction of the neutrons with the nucleus. The absorption cross-section for X-rays is much greater than that for neutrons. However, one should realize that, experimentally, it is the total absorption cross-section that is of importance. Therefore, a strongly scattering sample or a sample with a large incoherent scattering cross-section will effectively attenuate the radiation as well. In the calculation of the reflectivity, this would have to be taken into account in β.

For both X-rays and neutrons, contrast, or differences in the refractive index, can arise from variations in the mass density. In general, the range in mass density for polymers is small and the contrast, strictly from mass density variations, is not large. For X-rays the contrast is provided by the presence of higher atomic number elements where the number of electrons per unit volume can be large. With neutrons, on the other hand, the scattering length does not vary in a systematic manner with atomic number [12]. In fact, one of the largest differences in scattering lengths is that between two isotopes, the proton and the deuteron. The scattering lengths for deuterium and hydrogen are -0.374×10^{-12} cm and 0.667×10^{-12} cm, respectively. This large difference in the scattering lengths provides a unique means of labeling polymer molecules with minimal perturbation to the thermodynamics. For completeness it should be noted that, for magnetic materials, the nuclear spin can provide contrast when a polarized neutron beam is used. In general, though, this is not of great importance for polymers.

The complex part of the refractive index highlights an important difference between X-ray and neutron reflectivity. Here one is concerned with the absorption of the radiation by the sample. Consider two specific elements, namely carbon and silicon. The linear absorption coefficients of carbon are $0.0005\ \text{cm}^{-1}$ and $15.2\ \text{cm}^{-1}$, for neutrons ($\lambda \sim 3$ Å) and X-rays ($\lambda \sim 1.5$ Å), respectively, whereas in the case of silicon, the respective linear absorption coefficients are 0.004 and $141\ \text{cm}^{-1}$. Thus, it is evident that neutrons are much more penetrating than X-rays. As a result, using neutron reflectivity one can easily examine interfaces that are buried well within a sample, the structure of a polymer that is confined between two solid surfaces or the absorption of a polymer from solution onto a substrate. The fact that neutrons can pass through centimeters of a material without a substantial loss in flux is of tremendous value in the design of sample cells where in situ measurements are desired.

In vacuum, the component of the wave vector normal to the surface is given by

$$k_{z,0} = \frac{2\pi}{\lambda} \sin\theta, \tag{5}$$

where θ is the grazing incidence angle. The subscript z denotes the direction normal to the surface of the film and the subscript 0 denotes vacuum. If the reflected X-rays or neutrons are measured at an angle equal to the incidence angle, the diffraction vector is oriented normal to the surface, i.e. in the z direction. In a medium with a neutron scattering length density ρ^s (in the case of X-rays ρ^s is the product of r_0 times the electron density), the scattering vector in the medium is modified such that

$$k_{z,i} = (k_{z,0} - 4\pi\rho^s)^{1/2} = (k_{z,0}^2 - k_c^2)^{1/2}, \tag{6}$$

where k_c is the critical scattering vector which is given by $k_c = (2\delta)^{1/2}$.

It is the change in the refractive index or scattering vector from one medium to another that gives rise to reflectivity. This may occur at an interface between two dissimilar materials or from a continuous change in the scattering length density. In either case, a gradient in the scattering length density is required to reflect the radiation. The reflection coefficient at an interface between two media, i and $i+1$ is given [13, 14] by

$$r_{i,i+1} = \frac{k_{z,i} - k_{z,i+1}}{k_{z,i} + k_{z,i+1}}. \tag{7}$$

The reflectivity R is then given by

$$R = rr^*, \quad (8)$$

where r^* is the complex conjugate of r.

Consider a film on a substrate having a thickness d and uniform scattering length density. Here, there are two step changes in the reflection coefficients, at the air/film and film/substrate interfaces, separated by a distance d. The reflection coefficient of the sample, in terms of the reflection coefficients at the substrate/sample interface, $r_{1,2}$, and at the sample/air interface, $r_{0,1}$, can be written as

$$r = \frac{r_{0,1} + r_{1,2}\exp(2ik_{z,1}d)}{1 + r_{0,1}r_{1,2}\exp(2ik_{z,1}d)}. \quad (9)$$

The reflectivity can be shown to be

$$R(k_{z,0}) = \frac{r_{0,1}^2 + r_{1,2}^2 + 2r_{0,1}r_{1,2}\cos(2k_{z,1}d)}{1 + r_{0,1}^2 r_{1,2}^2 + 2r_{0,1}r_{1,2}\cos(2k_{z,1}d)}. \quad (10)$$

From Eq. (10) it is seen that, for a single film, the reflectivity profile as a function of $k_{z,0}$ will contain oscillations that are characteristic of the total film thickness. In fact, since the refractive indices for X-rays and neutron are only slightly less than unity, the film thickness is given by $\pi/\Delta k_{z,1}$. This represents a great advantage in comparison to techniques like ellipsometry where a precise value of the refractive index is needed to determine the film thickness.

The case of a homogeneous film on a substrate is one where the reflectivity can be solved analytically. In most situations one is dealing with a sample which has a continuous variation in the scattering length density and a simple analytic solution of the reflectivity does not exist. In addition, due to the loss of phase information, it is not possible to invert a reflectivity profile to determine the concentration gradients in the sample. Recently, there have been some advances made in the attempt to directly invert reflectivity data [15–20], though they have not, as of yet, been used extensively. Generally, one assumes a model concentration profile to calculate the reflectivity profile and compares this with the measured reflectivity profile. This represents one of the major disadvantages of reflectivity. The final model that one develops may or may not describe the actual concentration profile in the sample. In fact, many different models may be able to describe the same reflectivity profile! This underscores the need to couple reflectivity with other techniques, like X-ray photoelectron spectroscopy, dynamic secondary ion mass spectrometry or forward recoil spectrometry, to arrive at the proper concentration profile.

If it is assumed that one has a reasonable model of the concentration profile as a function of depth, then one calculates the reflectivity profile by converting the continuous function into a histogram where the step size in the histogram is arbitrary but sufficiently small to give a good approximation to the continuous function. Then, using Eq. (10) a recursion relation can be used to calculate the reflection coefficient of the n-layered histogram [21, 22]. For the first layer between the n and $n-1$ interface the reflection coefficient is

$$r_{n-1,n} = \frac{r'_{n-1,n} + r'_{n,n+1}\exp(2id_n k_n)}{1 + r'_{n-1,n}r'_{n,n+1}\exp(2id_n k_n)}, \quad (11)$$

where the prime denotes the reflectances at the respective interfaces given by Eq. (7). Using this reflection coefficient, the reflection coefficient of the next layer is given by

$$r_{n-2,n-1} = \frac{r'_{n-2,n-1} + r_{n-1,n}\exp(2id_{n-1}k_{n-1})}{1 + r'_{n-2,n-1}r_{n-1,n}\exp(2id_{n-1}k_{n-1})}. \quad (12)$$

Using this recursion relation one proceeds stepwise through the histogram calculating the reflection coefficient for each layer, finally ending with the reflection coefficient at the 0, 1 or air/sample interface. Since the reflection coefficient of each layer is dependent upon the reflection coefficients of the underlying layers, the reflection coefficient at the 0, 1 interface is that of the entire sample. Then, using Eq. (8), the reflectivity is calculated. Deviations between the calculated and measured reflectivity is minimized by systematically varying the scattering length densities and widths of the layers in the histogram.

An alternate means of describing the reflectivity that has been pioneered by Als-Nielsen [23] and coworkers is to write the reflectivity as

$$R(k_{z,0}) = \frac{k_c^4}{k_{z,0}^4}\left|\int \rho'(z)\exp(2ik_{z,0}z)\,dz\right|^2, \quad (13)$$

where k_c is the critical scattering vector and $\rho'(z)$ the normalized density gradient in the sample. The prefactor for the integral in Eq. (13) is the Fresnel reflectivity. This is the reflectivity that would be found if all the interfaces were sharp. At large $k_{z,0}$, the reflectivity varies by the inverse fourth power of $k_{z,0}$ which is analogous to Porod's law in small angle scattering. If the interface is rough, then one will get deviations from this behavior. For a Gaussian roughness at the air surface, Eq. (13) simplifies to

$$R(k_{z,0}) = R_F(k_{z,0})\exp(-4k_z^2\sigma^2), \quad (14)$$

where $R_F(k_{z,0})$ is the Fresnel reflectivity and σ is the standard deviation of the Gaussian function describing the roughness. From this equation it is obvious that reflectivity is very sensitive to the roughness of the sample. Even small roughnesses will cause a substantial deviation of the reflectivity from the Fresnel case.

One point that must be emphasized is that the concentration gradient that is determined from a reflectivity measurement represents a gradient that is averaged over the coherence length of the neutrons or X-rays. In general, this is on the order of microns. Consequently, from a simple specular reflectivity measurement, i.e. where the diffraction vector is

oriented normal to the surface of the film, it is not possible to distinguish between waviness at an interface or actual mixing of components at the interface. To do this, one needs to perform measurements where the diffraction vector is tilted away from the interface, i.e. where there is a component of the diffraction vector in the plane of the film. In this way, using a variety of theoretical arguments to describe the off-specular scattering [24–31], the height–height correlation function can be determined and, hence, provides a means of separating these two. Of course, if only mixing at the interface occurred, then there would be no off-specular scattering.

Finally, it is worthwhile to examine some of the advantages and disadvantages of using neutrons and X-rays. In the case of neutrons, isotopic labeling and deep penetration of the neutrons are advantageous. The deep penetration makes neutrons ideal for the investigation of interfaces buried within a sample. Neutrons used for scattering experiments have thermal energies, of order $k_B T$, and, hence, are "kind and gentle" [32]. This is of critical importance if one wants to observe changes in a sample as a function of time. One sample can be used repeatedly for kinetic studies. In addition, neutrons can be polarized which, for magnetic materials, is of considerable importance. Some of the disadvantages of neutrons are that the flux incident on the sample is low and for hydrogenous materials there is a considerable contribution to the background from incoherent scattering. These limit the measurement of neutron reflectivity to $\sim 10^{-6}$. After this, the background becomes comparable to or greater than the reflectivity. Thus, very thin films, ~ 20 Å or less, are difficult to measure with neutron reflectivity. In the case of X-rays, the major advantage is the high flux that one can deliver onto the sample. This comes, of course, with mixed blessings. While the high flux permits the measurement of the reflectivity down to 10^{-9} or less, radiation damage to the sample can be significant. One source of damage is by the generation of ozone by the X-ray beam near the surface in the presence of trace amounts of oxygen. Ozone aggressively oxidizes polymers. Damage can also come from the absorption of secondary electrons emitted when the substrate absorbs X-rays. Electrons are more strongly absorbed by the polymer and, hence, will cause more damage. There is an interesting twist here in that absorption of X-rays by the substrate strongly depends upon the atomic number of the substrate. Thus, the degradation of a sample by secondary electrons will depend upon the substrate and, for example, a sample may be destroyed on a Si substrate but not on a water surface. A second advantage of X-rays is that quite reasonable fluxes can be obtained from laboratory sources. Thus, a tremendous amount of information can be obtained without leaving the laboratory. The enhanced flux of X-ray sources and the low incoherent scattering of X-rays, make the measurement of off-specular scattering possible by X-rays but difficult by neutrons.

3. Reflectivity studies of polymers: An overview

The strength of reflectivity techniques lies in the ability to determine concentration gradients in materials with remarkable precision. As mentioned, the depth resolution of both X-ray and neutron reflectivity is ~ 5 Å. Recalling that the volume pervaded by a single polymer chain is on the order of hundreds of angstroms, reflectivity has provided the means of measuring changes in the concentration on the submolecular level. This unprecedented depth resolution has held the key to many different problems.

Consider first the simplest interface, i.e. between a polymer and air or vacuum. The angular dependence of the reflectivity provides a measurement of the surface roughness with extreme accuracy. The reflectivity is damped by an exponential square of the roughness and, consequently, measurement of the reflectivity at large angles provides a very accurate measurement of the surface roughness. One key feature that emerged from studies on the surface roughness is that amorphous polymers have a roughness comparable to their small molecule analogues [33–35]. While this feature seems obvious now, there was a considerable amount of controversy as to whether the large size of the polymer chains would give rise to an increased roughness. This is not the case and, within a monomer unit from the surface, the bulk density of the polymer is attained. As with small molecules, studies of the off-specular scattering, i.e. where there is a component of the diffraction vector in the plane of the film, have permitted the measurement of the amplitude and wavelength distribution of capillary waves on the surface. In the case of a glassy polymer, studies of this type have shown that capillary waves are frozen in at the glass transition temperature of the polymer [34–40].

Consider, now a little more complex problem, that is a mixture of two homopolymers or the solution of a homopolymer in a solvent. In general, the chemical difference between the two components is sufficient to cause a difference in the surface energies. This gives rise to a preferential affinity of one component to the free surface. Reflectivity has provided a unique means of quantitatively addressing, not only the surface excess of one of the components, but also the decay of the concentration to the bulk or solution concentration [41–55]. It should be noted that even in the case of a mixture of two polymers that are chemically identical but differ only in their labeling, one protonated and one deuterated, the labeling is sufficient to produce a slight difference in the surface energies and give rise to a preferential segregation of the deuterated component to the free surface [56, 57]. This slightly lower surface energy of the deuterated species has, in fact, hampered efforts to determine the spatial configuration of polymer chains near a free surface. If one considers a polymer chain where only the chain ends or chain centers are labeled with deuterium, neutron reflectivity would provide an ideal means of examining the dis-

tribution of different portions of the polymer chain in relation to the free surface. However, this slight biasing of the deuterated component to the surface can make isolation of strictly configurational effects difficult.

Consider now a mixture that is undergoing phase separation, i.e. the temperature of the mixture has been changed to bring the mixture into the envelope defined by the binodal in the phase diagram. Studies using neutron reflectivity, coupled with forward recoil spectroscopy, have beautifully shown that the phase separation is directed by the preferential segregation of one of the components to the free surface [58]. The surface excess pins fluctuations at the surface and tends to damp concentration fluctuations parallel to the surface [59]. Consequently, a layered structure emerges during the initial stages of the phase separation process. If, now, the sample is thin enough and the phase separation is allowed to proceed, then the phase separation can induce a roughening at the free surface due to a coarsening of the phases [60]. Whether or not roughening is evident will depend upon a balance between the interfacial tension between the phases and the difference in the surface energy of the components. Both X-ray and neutron reflectivity have been used, together with atomic force microscopy, to critically analyze this problem.

An even more subtle issue has emerged from reflectivity studies on polymer mixtures. If we consider that the preferential affinity of one component to the surface and, also, to the substrate interface, then the concentration of the polymer in the center of the film has changed. The magnitude of the change in the concentration will depend upon the sample thickness. The thinner the sample, the larger will be the change. Consequently, now the bulk of the sample is at a concentration that is different from the initial concentration, and, hence, the temperature at which phase separation occurs will be changed. Depending upon the initial concentration, this depletion of material could either promote or retard the phase separation of the mixture. In fact, recent reflectivity studies have borne this out [61, 62]. Finally, a problem that has not received much attention but is integrally related to the above is the effect of sample thickness on phase separation. In general, polymers phase separate via a spinodal phase separation process where, due to a balance between the thermodynamics and dynamics, the critical wavelength of the fluctuations is on the order of a tenth of a micron or more. Thus, if the sample thickness of a mixture is less than this, then there will be a suppression of the long wavelength fluctuation normal to the sample surface. This, should alter the characteristics of the phase separation and give a beautiful means of probing finite size scaling effects.

The behavior of polymer chains at the interface between a solid substrate and a solution or a polymer mixture has received a considerable amount of attention recently. In the case of bulk polymers, this interest has stemmed from gaining an understanding of the manner in which the adhesion between a polymer and a solid can be enhanced. Obviously, this has direct implications in filled polymer systems where mechanical properties of a composite is directly associated with cavitation at the interface between the polymer and the solid. In general, studies addressing this issue have focused on the segregation of one component in a mixture to the interface or to the segregation of a block copolymer to the interface where one of the blocks adheres to the substrate and the other block entangles with the matrix polymer [63, 64]. Using predominantly neutron reflectivity, coupled with ion beam scattering techniques, it has been possible to elucidate the amount of excess material at the interface and the amount of mixing of the absorbed component with the matrix material. In fact, if a diblock copolymer is used where the matrix material and the nonabsorbing block undergo a phase separation, then it has been shown that the extent of intermixing can be varied by a simple change in the temperature [65]. Thus, one can, conceivably, tailor the extent of entanglements between the absorbed block and the matrix and, therefore, tailor the mechanical properties to a specific need.

Much more attention has been paid to the absorption of a polymer chain onto the substrate from solution and on the concentration profile of a polymer chain anchored onto the solid surface. The polymer brush problem has now been studied by numerous groups using neutron reflectivity. Only recently, however, has a quantitative evaluation of the concentration profile been made with excellent agreement being obtained with simple mean field arguments [66–71]. More recently, efforts have been focusing on the effect of a flow field in altering the density profile. In particular, neutron reflectivity studies have been performed where the incident neutron beam is passed through a quartz or silicon substrate which constitutes one wall of the flow cell [72–75]. Probably the most striking result from such flow studies have been performed on micellar solutions [76]. Here, reflectivity studies have clearly shown that, in the flow field, the micelles order with respect to the surface and off-specular scattering studies performed in parallel show the ordering to be hexagonal.

Miscibility between two homopolymers is the exception as opposed to the rule. The small entropic gains on mixing such large molecules are easily off-set by slight nonfavorable interactions. The size of the domains formed during phase separation range from the micron scale to larger, depending upon the kinetics of the process. However, in many multicomponent applications, it is highly desirable to have one polymer dispersed in another where the size of the domains are small and where there is good adhesion between the dispersed phase and the matrix. Related to this is the issue of adhesion promotion between multilayered polymer structures. Here, due to the immiscibility of the homopolymers, adhesion between successive homopolymer layers is generally weak which can cause failures in applications. Copolymers,

however, can and have been used successfully to compatibilize homopolymers and to enhance adhesion [77–79]. Reflectivity studies have contributed significantly to the basic understanding of the behavior of copolymers at homopolymer interfaces [80, 81]. From reflectivity studies it has been possible to determine quantitatively the amount of copolymer segregated to the interface and the distribution of the copolymer segments at the interface. In addition, since the copolymer reduces the interfacial tension, the broadening of the interface, i.e. the enhanced mixing at the interface, has been examined in great detail. Current studies are now focusing on the effect of copolymer architecture on the effectiveness of the copolymer [82–86]. For example, rather than using diblock copolymers, triblock, random and grafted copolymers are being examined for this purpose.

One area that has received little attention but is quite worthy of investigation is a systematic investigation of the interfacial width in order to evaluate the segmental interaction parameter [87]. The interfacial width is directly proportional to the statistical segment length of the polymer and inversely proportional to the square root of the segmental interaction parameter. The stiffer the chain, i.e. the larger the statistical segment length, the broader will be the interface. Whereas the smaller the segmental interaction parameter, i.e. the more miscible are the two polymers, the broader will be the interfacial width. In general, the statistical segment lengths of polymers are known or can be measured easily by small angle scattering measurements. Consequently, a measurement of the interfacial width provides a direct measure of the segmental interaction parameter. Since the interfacial width can be measured with high precision, simple reflectivity studies provide an easy means of measuring χ. Thus, studies on a series of different polymer pairs or on one pair as a function of temperature provide access to information not accessible by other techniques. There is no question that the interfacial width can be determined from small angle scattering measurements. One simply needs to analyze the scattering at high scattering vectors and determine the deviation of the scattering from Porod's Law [88, 89], i.e. the asymptotic limit of the scattering at high scattering vectors for a system with infinitely sharp phase boundaries. However, extraction of the coherent scattering, requires subtraction of two small numbers. Thus, errors in the interfacial width determined by scattering are large. This, however, is not the case for reflectivity. One potential drawback to reflectivity is that concentration gradient determined by fitting the profile represents that variation in the scattering lengthens averaged over the coherence length of the neutron or X-ray. Therefore, capillary waves will contribute to the measured interfacial roughness. From specular scattering measurements alone, it is not possible to differentiate between intermixing and capillary waves. By measurements of the off specular scattering, though, it should be possible to distinguish between the two. Nonetheless, this simple measurement can provide a wealth of information on the temperature and molecular weight dependence of the segmental interaction parameter.

It is not possible to discuss exhaustively, all the different areas where reflectivity has had significant impact. However, some of the other areas where reflectivity has played a key role are

- Langmuir–Blodgett films [4, 90–93]
- Self-assembled monolayers [94–102]
- Surface induced ordering in diblock copolymers [103–109]
- Ordering of liquid crystals at surfaces [110–115]
- Confinement effects on polymers [116–119]
- Polymer/polymer interdiffusion [120–129]
- Surface mobility of polymers [130]
- Thermal expansion of homopolymers and multilayers [131, 132]
- Surface wetting [133–135]

In each of these cases either the high resolution of the technique, the ability to label a part of or an entire molecule, or the ability to probe a buried interface has been used. Consequently, reflectivity has provided a unique piece of information that was not accessible by other means.

Reflectivity has emerged as a premiere tool in the characterization of the surface and interfacial behavior of polymers. There are, however, some topics that are prime candidates for future study by specular reflectivity and off specular scattering where the impact of the results could be significant. These include

- Polyelectrolytes
- Ion containing polymers
- Polymers in well defined geometries
- Polymers at liquid/liquid interfaces
- Ion migration in polymer gels
- Nanofoam polymers
- Ordering of thin films under high electric fields
- Biopolymer membranes
- Selective absorption of biopolymers at surfaces
- Biocompatibilization of surfaces
- Lateral homogeneity of absorption processes
- Absorption onto heterogeneous surfaces

4. Diblock copolymers

The ordering of thin films of symmetric diblock copolymers on surfaces provides an ideal example to demonstrate some of the detail that can be obtained by reflectvity studies and has been a most interesting area of research. The specific copolymer that will be discussed here is that of polystyrene, PS, and poly (methyl methacrylate), PMMA. The copolymer will be designated as P(S-b-MMA). In cases where one of the blocks is perdeuterated, a "d" prior to the block will be used. For example, if the PS block is deuterated, the copolymer will be designated as P(d-S-b-MMA). This is an

ideal copolymer since the two components are quite similar. The glass transition temperature of PS and PMMA are 100° C and 115° C, respectively. The mass densities and statistical segment lengths of the two polymers are 1.05 g/cm^3 and 6.85 Å and 1.10 g/cm^3 and 7.1 Å, for PS and PMMA, respectively. The segmental interaction parameter is 0.029 and is only weakly dependent upon temperature and there is only a slight difference in the surface tension of the two. Despite these similarities, the behavior of the copolymer in thin films is markedly influenced by the presence of the substrate and air interfaces.

In the bulk a symmetric diblock copolymers will be either phase mixed or microphase separated into lamellar microdomains. When the product of the number of segments in the entire copolymer, N, and the segmental interaction parameter, χ, is less than 10.5, the copolymer will be phase mixed [136]. When $\chi N > 10.5$, the copolymer microphase separates. In the bulk, the transition from the disordered to ordered state has been shown to be a fluctuation induced first order phase transition [137, 138]. In most cases χ depends inversely on temperature; consequently, by cooling the copolymer in the bulk it can be driven from the disordered to the ordered state.

Shown in Fig. 1 is the neutron reflectivity of a P(d-S-b-MMA) film spin coated onto a thick silicon wafer, as a function of the neutron momentum normal to the surface, $k_{z,0}$. At small $k_{z,0}$ there is a region of total external reflection where all the neutrons incident upon the surface are reflected. Deviations from unity are related to geometric effects where the sample does not intercept the incident beam completely. At the critical angle, the neutrons penetrate into the sample and the reflectivity drops rapidly. However, there are distinct oscillations in the data, termed Kiessig fringes, which arise from interferences of neutrons reflected at the top surface of the film and the interface between the sample and substrate. From the separation distance between two successive fringes the sample thickness t can be determined directly from

$$t = \frac{\pi}{\Delta k_{z,0}}. \tag{15}$$

In this case, the sample thickness is calculated to be 1150 Å which compares well with the value of 1140 Å measured using optical ellipsometry. The solid line in the figure was calculated using the scattering length density profile shown in the inset which is essentially that of a film of a given thickness with no variation in the scattering length density as a function of depth. It is important to realize that the reflectivity results give no information on the phase state of the copolymer. The copolymer can be either phase mixed or microphase separated. If the latter is true, then, over the coherence length of the neutrons, the lamellar microdomains must be randomly oriented. The results do show that, for this copolymer, after spin coating, there is no preferential absorption of either component to the interfaces. The value

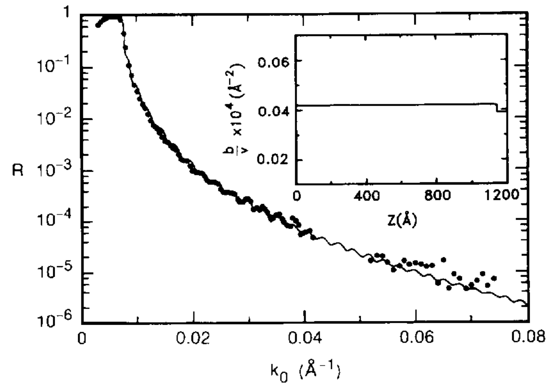

Fig. 1. Neutron reflectivity profile of a P(d-S-b-MMA) symmetric diblock copolymer spin coated onto a silicon substrate as a function of the neutron momentum normal to the surface. The sample was simply dried to remove residual solvent.

of the scattering length density used to calculate the reflectivity profiles is the weighted sum of the scattering length densities of the components, as would be expected. The roughness of the air/polymer interface, as determined from the damping of the reflectivity at large $k_{z,0}$, is 6 Å which is comparable to that seen for small molecule samples.

Shown in Fig. 2 is the reflectivity of a thin film, ~ 1500 Å, of P(S-b-d-MMA) having a molecular weight of ~ 3×10^4 after it has been heated to 176°C which is above the glass transition temperatures of the blocks and above the ordering transition temperature of the copolymer in the bulk. Near $k_{z,0} \sim 0.02$ Å^{-1} a first-order reflection is evident with indications of a very weak second order reflection. Thus, unlike the bulk copolymer, in the thin films there is clear evident of ordering. The scattering length density profile shown in the inset was used to calculate the reflectivity profile shown as the solid line in the figure. In terms of $\phi_{PS}(z)$, the volume fraction of PS segments a distance z from the surface, this scattering length density profile is given [117, 139] by

$$\phi_{PS}(z) = \max\left[\phi_A e^{-z/\xi}\cos\left(\frac{2\pi z}{L}\right),\; \phi_s e^{-(t-z)/\xi}\cos\left(\frac{2\pi(t-z)}{L}\right)\right] + \bar{\phi}_{PS} \tag{16}$$

where t is the sample thickness, L the period, ϕ_A and ϕ_s the excess concentrations of PS at the air and substrate interfaces, ξ the decay length and $\bar{\phi}_{PS}$ the average volume fraction of PS in the copolymer. From this model calculation, it is seen that PMMA, the more polar block, has absorbed more strongly onto the silicon oxide and PS, which has the lower surface energy, is preferentially located at the air surface. Thus, these preferential interactions of the blocks with the interfaces have induced an ordering of the thin films far above that seen in the bulk. The concentration fluctuations in the copolymer parallel to the interfaces have been suppressed, whereas those normal to the interface have been

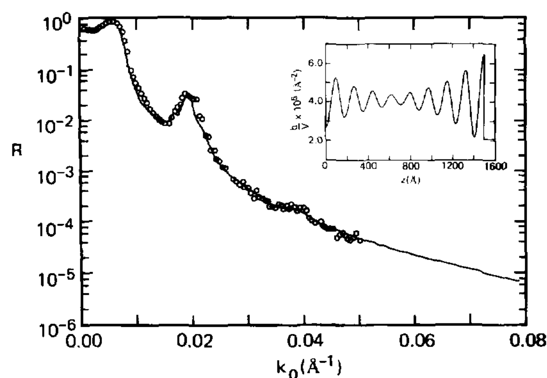

Fig. 2. Neutron reflectivity profile of a P(S-b-d-MMA) symmetric diblock copolymer as a function of the neutron momentum. The molecular weight of the copolymer is $\sim 3 \times 10^4$ and the sample was annealed at 176°C. The inset shows the scattering length density profile that yielded the best fit to the data, indicated by the solid line.

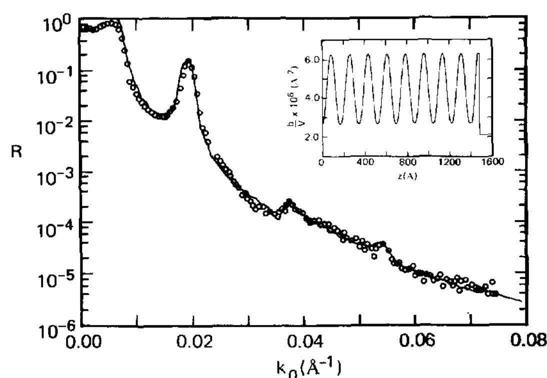

Fig. 3. Neutron reflectivity profile of the same copolymer as in Fig. 2 but the sample was annealed at 140°C. The inset shows the scattering length density profile that yielded the best fit to the reflectivity profile, the solid line in the figure.

enhanced. The most critical parameter that is derived from these studies is the decay length. The closer one is to the ordering transition, the greater will be the decay length. By decreasing the annealing temperature of the film to 140°C, i.e. below the bulk order to disorder transition temperature, the reflectivity profile, as shown in Fig. 3, changes markedly. In these data the first-order reflection has intensified and sharpened significantly and the higher order reflections are much more pronounced. The scattering length density profile shown in the inset, characteristic of a fully ordered diblock copolymer, was used to calculate the reflectivity profile. By performing a series of studies as a function of the temperature, the temperature dependence of the decay length can be determined. The temperature at which the decay length become infinite, can be taken as the ordering transition temperature of the copolymer. Studies performed as a function of the film thickness will then provide a measurement of the effect of sample thickness or finite sample size on the ordering transition temperature. It has been shown that the ordering transition temperature scales with the t^{-3}, a result that is in accord with finite size scaling arguments developed for small molecules [140–142].

An interesting question that arises is the phase of the concentration waves propagating into the bulk from the surface. In the case where each component of the block is located preferentially at one of the interfaces, if the sample thickness is $(n + \frac{1}{2})L$, where n is an integer, then the two waves will be in phase with one another. However, if the sample thickness deviates from this, then the waves will be out of phase and tend to destructively interfere with one another in the center. This should, in principle, cause a suppression of the ordering in the films and, hence, a suppression of the ordering transition temperature. Therefore, as the film thickness decreases, one would expect that the ordering transition temperature of the copolymers should exhibit an oscillatory behavior. This is currently under study [143].

An alternate means of driving the copolymer into the ordered state is to increase the molecular weight. Shown in Fig. 4 is the reflectivity profile of P(d-S-b-MMA) film ($\sim$ 1500 Å in thickness) with a molecular weight of 10^5 after the film was heated to 175°C. The multiple Bragg reflections seen in the reflectivity profile are a direct consequence of the self assembly of the diblock copolymer into a multilayered structure. By increasing the molecular weight of the copolymer, the period has increased which shifts all the reflections into smaller $k_{z,0}$, and the copolymer is strongly microphase separated which increases the purity of the phases. This enhances the contrast of the domains which causes the peaks to be more intense. In fact, the first-order peak has a reflectivity close to unity.

One of the true strengths of reflectivity is that the technique is most sensitive to gradients in the scattering length density or concentration. The scattering length density profile shown in the inset was used to calculate the solid line in the figure. As can be seen, agreement between the calculated and measured reflectivity profiles is quite good over the entire $k_{z,0}$ range. To produce a good fit to the data an interfacial width a_I, of 50 Å was required. The interfacial width is given by

$$a_I = (2\pi)^{1/2}\sigma, \tag{17}$$

where sigma is the rms roughness of the interface defined in Eq. (14). Variation of a_I by more than ± 2 Å caused the calculated reflectivity to deviate substantially from the measured profile. The precision to which the interfacial width can be measured is extremely important. Usually, the interfacial width between domains was determined from either small angle X-ray or neutron scattering measurements where the broadening of the interface causes a suppression of the scattering at large scattering vectors. However,

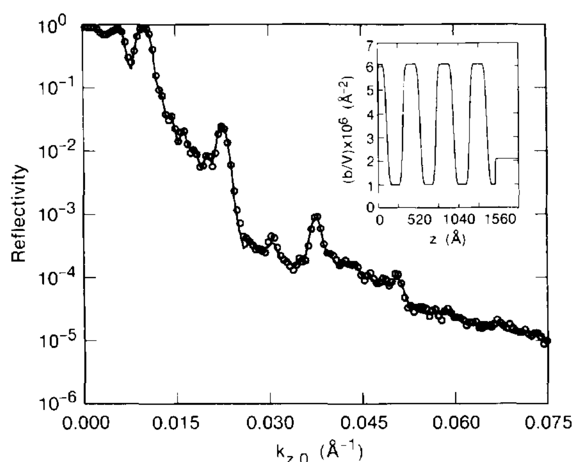

Fig. 4. Neutron reflectivity profile of a P(d-S-b-MMA) diblock copolymer as a function of the neutron momentum where the copolymer molecular weight is $\sim 10^5$ and the copolymer was annealed at 175°C. The solid line in the figure is the best fit to the reflectivity profile using the scattering length density profile shown in the inset.

obtaining a precise value by this means is difficult since the scattering is inherently weak and the subtraction of the background is problematic. The precision that reflectivity offers is unsurpassed which, in the case of polymers, is important since the interfacial width is related to fundamental quantities of the segmental interaction parameter and the statistical segment length.

Coupling the resolution capabilities of reflectivity with the multilayering of the copolymer microdomains, and the ability to synthesize molecules with specific labeling, allows one to obtain even more detailed information on the conformation of the copolymer chains. For example, consider the schematic diagrams shown in Figs. 5(a) and (b). In these examples there is a diblock copolymer multilayer where most of the copolymer is protonated but specific portions of the chain are labeled with deuterium. In Fig. 5(a) only the junction points of the copolymer are labeled and in Fig. 5(b) only the chain ends of one of the blocks are labeled with deuterium. To the right of each profile is a schematic representation of the variation in the concentration of the deuterated segments in the copolymer. Even though the concentration of the deuterated segments is less than 2%, the multilayering of the structure will enhance the ability to discern the distribution of the chain segments by producing interferences. As a result, the spatial distribution of the different portions of the chains can be determined by reflectivity in a fairly direct manner [144].

Shown in Fig. 6 is the reflectivity profile of an ordered copolymer multilayer where only a few segments of PS at the junction points were labeled with deuterium. In the raw data one can see interferences arising from the multilayered

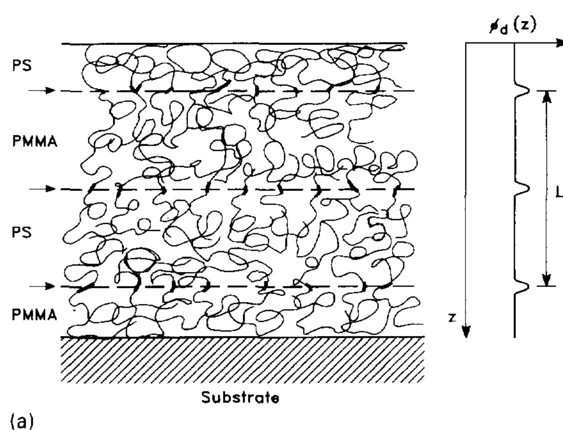

Fig. 5. (a) Schematic diagram of a diblock copolymer that is ordered into a multilayer but only the junction points of the copolymer are labeled with deuterium.

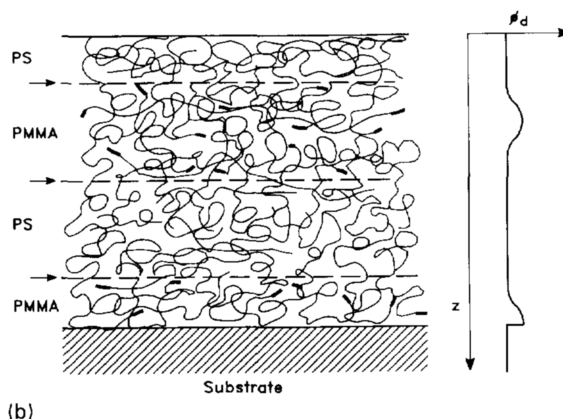

Fig. 5. (b) Schematic diagram of a diblock copolymer that is ordered into a multilayered structure where the ends of one of the blocks have been labeled with deuterium.

structure even though only a small fraction of the segments are labeled. The scattering length density profile shown in the inset was used to calculate the solid line in the figure. From the scattering length density profile it is immediately seen that the junction points are highly localized at the interfaces between the PS and PMMA microdomains. By combining this scattering length density profile with that obtained from the case where all the PS segments are labeled with deuterium, the concentration and distribution of all of the components in the copolymer are defined. This is shown in Fig. 7 where the concentration of the PS segments in the copolymer is shown as the dotted line, the junction points as the dashed line and the PMMA segments as the solid line. Mean field calculations were performed on this copolymer using the known statistical segment lengths and χ and the agreement between the two was exceptionally good [145].

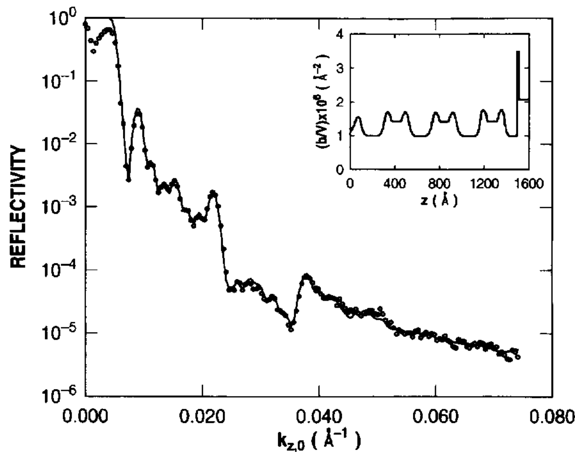

Fig. 6. Neutron reflectivity profile of a P(S-b-MMA) diblock copolymer having a molecular weight of $\sim 10^5$ where $\sim 2\%$ of the styrene units adjacent to the junction points have been labeled with deuterium. The scattering length density profile shown in the inset yielded the best fit to the reflectivity profile shown as the solid line.

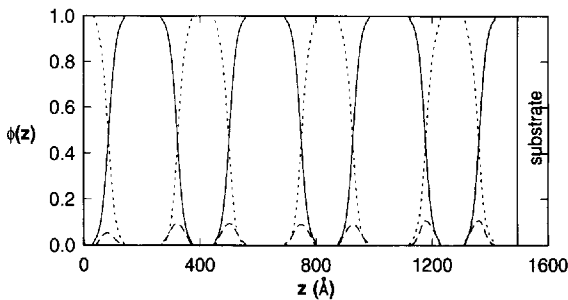

Fig. 7. The variation in the concentration of the styrene segments of the copolymer, the methylmethacrylate segments of the copolymer and the copolymer junction points as a function of depth in the sample. These concentration profiles were obtained from the scattering length density profile shown in Fig. 6 along with the scattering length density profile obtained from the case where the entire PS block of the copolymer was labeled with deuterium.

The ability to label chains with deuterium has opened a large number of possible studies. For example, studies on mixtures of copolymers having different molecular weights were performed where one of the blocks, say the PS block of the lower molecular weight copolymer, was labeled with deuterium. This permitted the examination of the spatial distribution of the lower molecular copolymer in the high molecular weight host [146]. It was quantitatively shown that the lower molecular weight copolymer was segregated to the interfacial region, whereas the higher molecular weight copolymer occupied the central region of the lamellar microdomain preferentially. Studies on mixtures of homopolymers with diblock copolymers [147, 148] have shown that the homopolymer is incorporated into the multilayered structure provided the molecular weight of the homopolymer does not substantially exceed the block copolymer molecular weight. With increasing homopolymer molecular weight, the localization of the homopolymer to the central portions of the lamellar microdomain increases. In cases where the homopolymer molecular weight is much greater than the copolymer molecular weight, then the homopolymer is excluded from the multilayered structure and macrophase separation occurs. One can also make a bilayer of copolymers having the same molecular weight where one of the copolymers is perdeuterated. By examining the change in the scattering length density with time, one can measure the interdiffusion of chains through the lamellar microdomains normal to the interface [149]. These are a few examples of the many different studies that can be performed on these multilayers to examine fundamental aspects of symmetric diblock copolymers using reflectivity methods.

Up to now we have focused on the use of neutron reflectivity to study the multilayering of the copolymers. However, X-ray reflectivity on these systems can also be used to provide unique information. Shown in Fig. 8 is the X-ray reflectivity profile as a function of $k_{z,0}$ obtained for a P(S-b-MMA) copolymer after it has been annealed at 170°C. At low values of $k_{z,0}$ the data gradually increases and near 0.01 Å^{-1} a drop in the data is seen. With increasing $k_{z,0}$, the data increase slightly, then drop markedly. At higher values of $k_{z,0}$ cusps are seen in the data. Superposed on the entire reflectivity profile is a low amplitude, high frequency oscillation. At low values of $k_{z,0}$, the gradual increase in the data is due to the incomplete interception of the incident beam by the substrate. As the incidence angle increases, more of the beam is subtended and, consequently, the reflectivity increases. The first drop in the reflectivity is due to the critical angle of the copolymer, $k_{c,p}$. Slightly above this, the X-rays penetrate into the sample and are absorbed by the polymer, but there is total reflection at the Si interface. At the critical angle of the Si, $k_{c,Si}$, the reflectivity begins to decrease rapidly. The low amplitude, high frequency oscillations in the data arise from the total film thickness, whereas the cusps are constructive interferences originating from the slight electron density differences between the PS and PMMA layers in the multilayer. These interferences can be seen more clearly in Fig. 9 where the region around the third- and fifth-order reflections have been magnified. From these data alone, without a detailed analysis of the reflectivity profile, the total thickness of the sample can be determined from $\Delta k_{z,0}$ between two successive minima. In this case, the total thickness is 5560 Å. From the position of the multilayer reflections, the period of the copolymer is found to be 445 Å. Consequently, this film is a multilayer containing exactly 12.5 layers. Using only these parameters two different investigations have been performed. In the first, the thermal expansion of the multilayers was measured [132]. If one thinks about this problem, one is faced with a

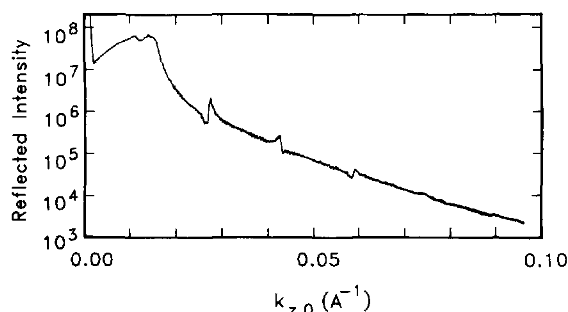

Fig. 8. X-ray reflectivity profile of a P(S-b-MMA) diblock copolymer that has self-assembled into a multilayered structure as a function of the $k_{z,0}$. The critical angles of the copolymer, $k_{c,p}$, and the silicon substrate, $k_{c,Si}$, are indicated.

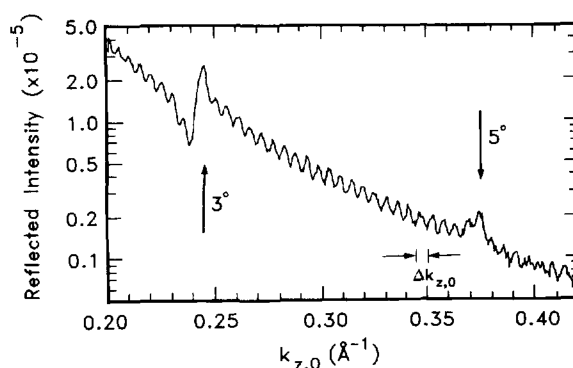

Fig. 9. Expansion of the X-ray reflectivity profile of a P(S-b-MMA) diblock copolymer in the vicinity of the third- and fifth-order reflections.

dilemma. First, since the copolymer is confined to the substrate, then as the sample is heated all the thermal expansion must occur in a direction normal to the surface. Thus, rather than the thickness increasing according to the linear thermal expansion coefficient, it expands by three times that quantity. For a simple homopolymer layer, this does not create any severe problems. However, for a multilayered structure, where the junction points of the copolymers are confined to the interfaces between the microdomains, this causes a stretching of the copolymer chains at the interface. If the expansion was only by the linear thermal expansion coefficient, then the stretching of the chains would be identical to that seen in the bulk. However, since the expansion is by three times that amount, the copolymer chains, for any temperature above the glass transition temperature are stretched three times too much. This excess stretching causes a storage of elastic energy in the chain which must be relieved for the copolymer to be at equilibrium. The manner in which the copolymer responds is by forcing chains through the multilayered structure, onto the free surface. This creates more space at the interfaces for the copolymer chains, whereupon the chains can relax to an equilibrium state. This relaxation process requires that there is a balance between the elastic retractive force of the chain and the energy required to mix the incompatible blocks. Evidence is seen for this mechanism when one observes the period of the copolymer as a function of temperature and time. In this case, the period is seen to increase according to the volume expansion coefficient. However, holding the sample at a specific temperature results in a gradual decrease in the period. Cooling the sample results in a decrease in the period according to the volume expansion coefficient, but holding the sample at a specific temperature after cooling results in a gradual increase in the period as chains are pulled back into the multilayer.

A second study where X-ray reflectivity has proven to be valuable utilizes the same features in the reflectivity profile. Consider now the situation where the copolymer film deviates slightly from the $(n + \frac{1}{2})L$ condition. This essentially places a small amount of frustration on the multilayered structure in that each chain must stretch or compress a to compensate for the imposed thickness constraint [150]. If the initial thickness is much different from the $(n + \frac{1}{2})L$ constraint, then islands or holes will form on the surface, as mentioned previously. In fact, if the period of the copolymer is examined where there is a slight frustration, then one observes a deviation in the period and the free surface of the film is truly acting as a confining wall. The amount of frustration or change in the period that is observed will, of course, depend upon the number of layers in the multilayer. The greater the number of layers, the less each copolymer chain will have to expand or contract to compensate for the frustration. This effect is clearly seen in the X-ray reflectivity profiles. However, it is found to be only a quasi-equlibrium condition for, with time, the period is found to gradually return to its equilibrium structure. To give a feeling of the time scales involved, usually with a P(S-b-MMA) copolymer having a weight average molecular weight of 10^5, the self assembly into a multilayered structure occurs within a matter of hours. However, when the film thickness deviates only slightly from the ideal condition, the relaxation back to the equilibrium structure occurs over a time scale of weeks. Consequently, one can consider the free surface as an effective solid wall, initially (see Fig. 10).

In all of the studies up to now the free surface has provided a route to relieve frustration, imposed by sample thickness. If, however, the sample is confined between two impenetrable surfaces, then the copolymer must modify its morphology in some manner to relieve the frustration. For example, the orientation of the lamellar microdomains may change or the fundamental repeat of the copolymer may change to relieve the imposed frustration. Confinement of any polymer can be accomplished in a fairly simple manner [116, 118, 119, 151]. Spin coating a polymer onto a solid substrate results in a film of uniform thickness over very large areas with negligible roughness at the free surface. If

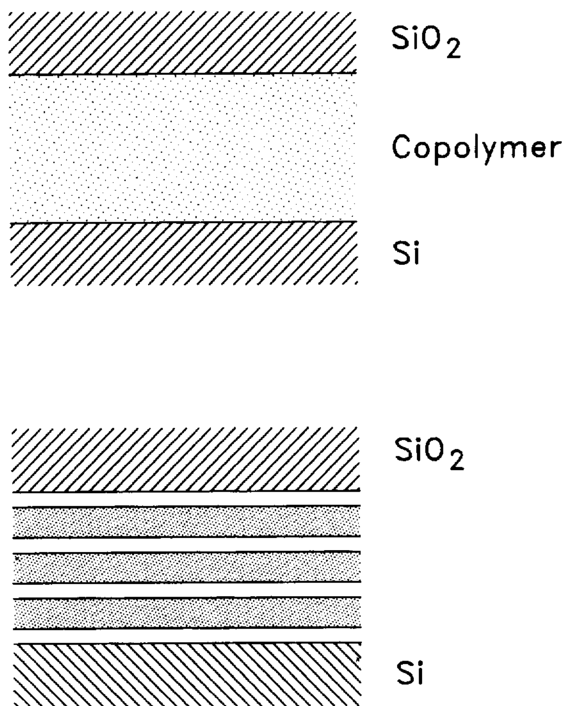

Fig. 10. Schematic diagrams of a copolymer confined between two solid barriers. In the first case, the copolymer is disordered and in the second case the copolymer is ordered into a multilayered structure between the barriers.

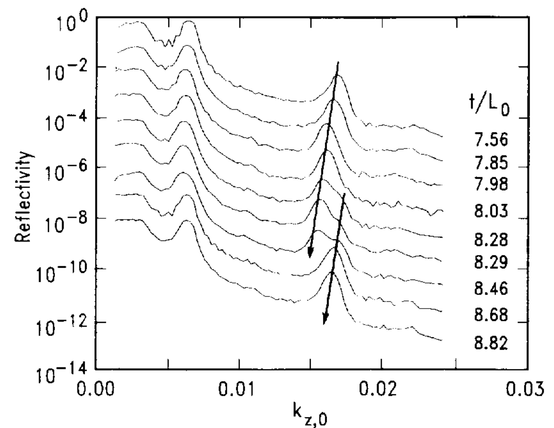

Fig. 11. Neutron reflectivity profiles of a P(d-S-b-MMA) diblock copolymer confined between two surfaces where the separation distance has been changed. The separation distance is indicated by the reduced separation distance, t/L_0, where t is the thickness and L_0 is the equilibrium period of the copolymer.

a thick layer of SiO_x is evaporated onto the surface of the film, such that the SiO_x layer is mechanically strong, then the copolymer is effectively confined between two parallel, oxide layers. Variation in the separation distance between the layers can be done by preparing a separate sample with a different thickness. While such a procedure is work intensive, it accomplishes the desired end very effectively. It has, in general, been found that during the evaporation the silicon oxide can chemically react with the polymer. Consequently, we have used a very thin (~ 50 Å) layer of high molecular weight PMMA on top of the copolymer to protect the underlying copolymer while maintaining a strong preferential attraction for the PMMA block of the copolymer.

It is worth noting that neutron reflectivity offers the only means, at present, of investigating the variation in the concentrations of components as a function of the distance between two confining surfaces. While one can use synchrotron radiation to probe the structure of confined materials, the attenuation of the X-rays is substantial in a reflection experiment when the path length of the X-rays is considered. Neutrons, on the other hand, can penetrate through either the SiO_x overlayer or through the Si substrate without a substantial loss in the flux.

The effectiveness of the confinement is manifest in the reflectivity data shown in Fig. 11. Shown are the profiles for P(S-b-d-MMA) where the film thickness, indicated on the right as t/L, was gradually increased [116, 119]. The appearance of distinct Bragg reflections in the data demonstrate convincingly that the orientation of the lamellar microdomains has not changed and remains parallel to the confining interfaces. Focusing on the third order Bragg reflection, as the separation distance between the walls increases, the maximum shifts into smaller $k_{z,0}$, i.e. the period increases, with increasing separation distance. This means that the copolymer chains contract or stretch to compensate for the imposed frustration. However, the increase in the period does not continue indefinitely. Slightly above a reduced thickness of 8.25, a second peak begins to emerge at higher $k_{z,0}$, i.e. a shorter period begins to appear. With increasing separation distance, this shorter period dominates and then, begins to increase with increasing separation distance. Consequently, there is a cyclic expansion and compression of the copolymer chains in response to the continued increase in the separation distance.

As a direct consequence of the periodic change in the period, the number of layers confined between the two surfaces must change. Shown in Fig. 12 is the total film thickness divided by the measured period, t/L, as a function of the film thickness divided by the equilibrium, t/L_0. Here it is seen that t/L, i.e. the number of layers confined between the two surfaces, is always an integer. As the film thickness increases, the number of periods goes through a first order transition where at half integer values of t/L_0, i.e. at the point of maximal frustration, the number of layers changes discontinuously by one. This discrete change in the number of steps persists over a very large range in the separation distance. With an increase in the number of layers, the frustration experienced by each layer decreases. Therefore, the

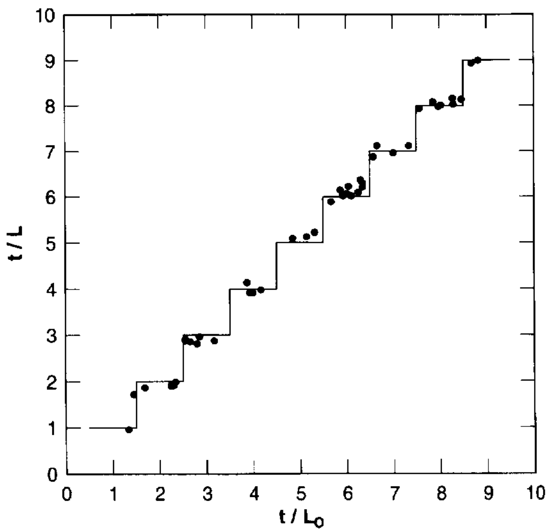

Fig. 12. The number of periods confined between two solid surfaces, t/L, for a P(d-S-b-MMA), as a function of the reduced film thickness, t/L_0. The solid line is a simple step function which describes the variation in the number of periods quite well. Note that the changes in t/L are essentially first-order with respect to t/L_0 where changes occur at half-integer values of t/L_0. These thicknesses correspond to the points of maximal frustration.

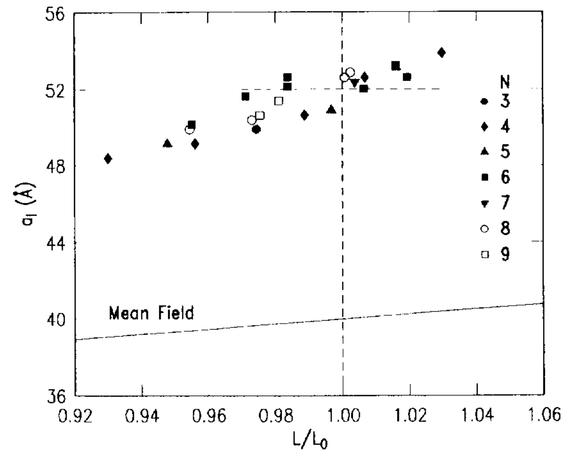

Fig. 13. The variation in the interfacial width as a function of the reduced period, L/L_0, for copolymer multilayers confined between two solid surfaces. The numbers at the right correspond to values of t/L, i.e. the number of period confined between the surfaces. The solid line is the interfacial width determined from self-consistent mean field calculations.

expansion or compression of each layer decreases in proportion to $1/n$ with increasing separation distance. Thus, the copolymer responds to the imposed frustration by stretching or compressing the individual copolymer chains at the interface. When the chain stretching become too large, i.e. the stored elastic energy becomes greater than the energy required to create two new copolymer interfaces, then an additional layer is formed with the copolymer compressing.

A more detailed analysis of the reflectivity profiles of the confined copolymers yields information on the interfacial width between the successive layers. Shown in Fig. 13 are the interfacial widths plotted as a function of the reduced period. The intersection of the two dashed lines represents the equilibrium interfacial width corresponding to the bulk equilibrium structure. From these data it is seen that the interfacial widths of compressed multilayers are less than the unperturbed value, whereas those for the expanded layers are greater than the unperturbed value. Also, to within experimental errors, the data reduce to one curve regardless of the number of confined layers. The solid line in the figure represents the result obtained from self-consistent mean field calculations [152, 153]. As can be seen, even under the condition of zero frustration, there is a substantial deviation between the calculated and measured result. One possible explanation for this is capillary waves [154]. Recalling that the scattering length density profile obtained is laterally averaged over the coherence length of the neutrons, then the amplitude of the capillary waves having wavelengths less than the coherence length of the neutrons would contribute to the measured width. If we assume that the contributions from the two add in quadrature, [145] then

$$(a_I)_{\text{meas}} = [(a_I)^2_{\text{MF}} + 2\pi\langle(\Delta z)^2\rangle]^{1/2}, \tag{18}$$

where a_{MF} is the mean field interfacial width and (Δz) is the amplitude of the capillary waves. The average mean squared amplitude of the capillary waves is given by

$$\langle(\Delta z)^2\rangle = \frac{k_B T}{2\pi\gamma_{AB}} \ln\left(\frac{\lambda_{\max}}{\lambda_{\min}}\right), \tag{19}$$

where γ_{AB} is the interfacial tension between the PS and PMMA, $\lambda_{\max}$ and $\lambda_{\min}$ are the maximum and minimum cut-off wavelengths. An upper limit to $\lambda_{\max}$ can be taken as the period of the copolymer. The minimum wavelength can be taken as the neutron wavelength. Substitution into Eq. (19) yields $2\pi\langle(\Delta z)^2\rangle = 28$ Å. This, coupled with the mean field result, $a_I = 40$ Å, yields $a_I = 49$ Å, which is in precise agreement with the measured value at equilibrium. Thus, one likely explanation for the variation in the interfacial width with the separation distance is that when the period is compressed, the capillaries waves are suppressed in amplitude. However, when the period is expanded, the amplitude of the capillary waves is increased.

Currently, efforts in diblock copolymers are focusing on the ability to control the orientation of the microstructure. In fact, some success has been achieved by the use of a random copolymer at the two interfaces where the concentration of the random copolymer can be varied across the entire composition range [155]. This effectively allows one to change the potential that the surface is presenting to the

copolymer. By balancing the interaction of the copolymer segments, the interaction of the copolymer segments with the two interfaces can, under certain conditions, cause the orientation of the lamellae to be vertical [156–158]. In a similar vein, electric fields are, also, being used to control the orientation of the microstructure [159–161]. It should be noted that in thick films, electric fields are not an effective way to align diblock structures. However, in thin films, only small voltages are required to generate massive fields and, hence, more likely to align the copolymer structure. Having the ability to make copolymers do what you wish, will inevitably, lead to significant advances in the use of diblock and multiblock copolymers. Given the power of reflectivity, there is no question that it will continue to be used as a decisive means of probing the copolymer morphology.

5. Conclusion

In this article a brief review of the basic principles of reflectivity has been presented highlighting some of the key aspects of the technique. Some of the areas where reflectivity methods have made and are continuing to make significant contributions in the investigation of polymers were outlined. Finally, a review of a systematic series of investigations on the surface ordering of block copolymers was presented. In this case, the strengths of neutron and X-ray reflectivity were brought to bear on the interesting behavior of the self-assembly of symmetric diblock copolymers. Reflectivity techniques, coupled with the ability to selectively label either a part of or the entire block copolymer molecule, have helped define the morphology and conformation of diblock copolymer molecules with unprecedented detail. In addition, reflectivity methods have permitted the investigation of phenomena, as for example phase transitions in confined geometries, which are not accessible by other techniques. These studies, in turn, have opened the door to many other aspects on the ordering behavior of diblock copolymers.

As a closing remark it is imperative to reiterate that, while reflectvity methods are powerful, they must be used in conjunction with other techniques to fully realize their potential. Many models can be used to describe a single reflectivity profile. Thus, it is always best to have some idea as to the general behavior of a material first as would be provided by, for example, ion beam techniques. Then, reflectivity can be used quantitatively to describe the concentration profiles in a sample. Without such information, one can easily be led astray in the evaluation of the reflectivity data. In cases where such additional information is not available, the proper design of an experiment, as, for example, labeling different parts of the molecules or by changing the contrast in the system, is necessary to define the concentration profile quantitatively.

Acknowledgements

The author wishes to express his sincere gratitude to G. Coulon, S.H. Anastasiadis, A.M. Mayes, A. Menelle, P. Bassereau, P. Lambooy, P. Mansky, S.K. Satija, C.F. Majkrzak, Z. Cai and S.K. Sinha (a.k.a. "The Bhagwan") with whom the studies on the diblock copolymers have been done over the past few years. For me, these collaborations have been a true learning experience and I am thankful to have had the opportunity to work with them. I am greatly indebted to G.P. Felcher who introduced me to reflectivity. Finally, I would like to acknowledge the partial support of the US Department of Energy, Office of Basic Energy Sciences under contract FG03-88ER-45375.

References

[1] J.B. Hayter, R.R. Highfield, B.J. Pullman, R.K. Thomas, A.I. McMullen and A. Penfold, J. Chem. Soc. Faraday Disc. 77 (1983) 1437.
[2] R.R. Highfield, R.K. Thomas, P.G. Cummins, D.P. Gregory, J. Mingins, J.B. Hayter and O. Scharpf, Thin Solid Films 99 (1983) 165.
[3] R.R. Highfield, R.P. Humes, R.K. Thomas, P.G. Cummins, D.P. Gregory, J. Mingins, J.B. Hayter and O. Scharpf, J. Coll. Interface Sci. 97 (1984) 367.
[4] M. Pomerantz and A. Segmueller, Thin Solid Films 68 (1980) 33.
[5] R.M. Niklow, M. Pomerantz and A. Segmüller, Phys. Rev. B 23 (1981) 1081.
[6] T.P. Russell, Mater. Sci. Rep. 5 (1990) 171.
[7] J. Penfold and R.K. Thomas, J. Phys.: Condens. Matter 2 (1990) 1369.
[8] M. Stamm, Adv. Polym. Sci. 100 (1991) 4.
[9] M. Deutsch and B. Ocko, Encyclopedia of Appl. Phys., in press.
[10] X. Zhou and S. Chen, Phys. Rep. 257 (1995) 223.
[11] M. Born and E. Wolf, Principles of Optics (Pergamon Press, Oxford, 1980; 6th ed.).
[12] G.E. Bacon, Neutron Diffraction (Clarendon Press, Oxford, 1975).
[13] O.S. Heavens, Optical Properties of Thin Solid Films (Butterworths, London, 1955).
[14] J. Lekner, Theory of Reflection (Nijhoff, Dordrecht, 1987).
[15] N. Berk and C.F. Majkrzak, Phys. Rev. B 51 (1995) 11 296.
[16] C.F. Majkrzak and N. Berk, Physica B 221 (1996) 520.
[17] V.O. de Haan, A.A. van Well, S. Adenwella and G.P. Felcher, Physica B, in press.
[18] B. Carvalho and S.H. Chen, Phys. Rev. E 47 (1993) 743.
[19] X.L. Zhou, S.H. Chen and G.P. Felcher, Phys. Rev. A 46 (1992) 1839.
[20] S.K. Sinha, M.K. Sanyal, K.G. Huang, A. Gibaud, M.H. Rafailovich, J. Sokolov, X. Zhao and W. Zhao, in: Surface X-ray and Neutron Scattering, eds. H. Zabel and I.K. Robinson (Springer, Berlin, 1992) p. 85.
[21] L.G. Parratt, Phys. Rev. 95 (1954) 359.
[22] L.G. Parratt, J.Chem. Phys. 53 (1956) 597.

[23] J. Als-Nielsen, in: Structure and Dynamics of Surfaces, II. Phenomena, Models and Methods, eds. W. Schommers and P. von Blanckenhagen (Springer, Berlin, 1987).
[24] S.K. Sinha, E.B. Sirota, S. Garoff and H.B. Stanley, J. Chem. Phys. 78 (1988) 1611.
[25] R. Pynn, Physica B180/181 (1992) 465.
[26] R. Pynn, Physica B173 (1991) 71.
[27] P. Beckmann and A. Spizzichino, The Scattering of Electromagnetic Waves from Rough Surfaces (Pergamon Press, Oxford, 1963).
[28] Wen-li Wu, J. Chem. Phys. 98 (1993) 1687.
[29] Wen-li Wu, J. Chem. Phys. 101 (1994) 4198.
[30] Z. Cai, K. Huang, P.A. Mantano, T.P. Russell, J.M. Bai and G.W. Zajac, J. Chem. Phys. 98 (1993) 2376.
[31] G.P. Felcher, R.J. Goyette, T.P. Russell, S.H. Anastasiadis, M. Foster and F.S. Bates, Phys. Rev. B 50 (1994) 9565.
[32] S.K. Sinha, private communication.
[33] W. Jark, T.P. Russell, G. Comelli and J. Stöhr, Thin Sol. Films 170 (1989) 309.
[34] M.K. Sanyal, S.K. Sinha, K.G. Huang and B.M. Ocko, Phys. Rev. Lett. 66 (1991) 628.
[35] X.Z. Wu, E.B. Sirota, S.K. Sinha, B.M. Ocko and M. Deutsch, Phys. Rev. Lett. 70 (1993) 958.
[36] X. Zhao, W. Zhao, J. Sokolov, M.H. Rafailovich, M.K. Sanyal, S.K. Sinha, B.H. Cao, M.W. Kim and B.B. Sauer, J. Chem. Phys. 97 (1992) 8536.
[37] D.K. Schwartz, M.L. Schlossman, E.H. Kawamoto, G.J. Kellogg, P.S. Pershan and B.M. Ocko, Phys. Rev. A 41 (1990) 5687.
[38] P.S. Pershan, Faraday Disc. 89 (1990) 231.
[39] G.J. Kellogg, P.S. Pershan and B.M. Ocko, Phys. Rev. A 41 (1990) 5687.
[40] B. Cull, S. Tushan, S. Kumar, R. Shih and J. Mann, Phys. Rev. E 51 (1995) 526.
[41] R.A.L. Jones, L. Norton, E.J. Kramer, R.J. Composto, R.S. Stein, T.P. Russell, A. Mansour, A. Karim, G.P. Felcher, M.H. Rafailovich, X. Zhao and S. Schwarz, Eutrophys. Lett. 12 (1990) 41.
[42] X. Zhao, M.H. Rafailovich, J. Sokolov, R.A.L. Jones, E.J. Kramer and S.A. Schwarz, Macromol. 24 (1991) 5991.
[43] J. Sokolov, M.H. Rafailovich, R.A.L. Jones and E.J. Kramer, Appl. Phys. Lett. 54 (1989) 590.
[44] R.J. Composto, R.S. Stein, A. Mansour, A. Karim and G.P. Felcher, Physica B 156/157 (1989) 434.
[45] R.J. Composto, R.S. Stein, G.P. Felcher, A. Mansour and A. Karim, Mater. Res. Soc. Symp. 166 (1990) 485.
[46] R.A.L. Jones and E.J. Kramer, Polymer 34 (1993) 115.
[47] E.M. Lee, E.A. Simister and R.K. Thomas, Mol. Cryst. Liq. Cryst. 179 (1990) 151.
[48] M.S. Kent, L.T. Lee, B. Farnoux and F. Rondelez, Macromol. 25 (1992) 6240.
[49] P.M. Saville, I.R. Gentle, J.W. White, J. Penfold and J.R.P. Webster, J. Phys. Chem. 98 (1994) 5935.
[50] L.T. Lee, E.K. Mann, O. Guiselin, D. Langevin, B. Farnoux and J. Penfold, Macromol. 26 (1993) 7046.
[51] J.F. Ellman, B.D. Johs, T.E. Long and J.T. Koberstein, Macromol. 27 (1994) 5341.
[52] X. Sun, E. Bouchard, A. Lapp, B. Farnoux, M. Daoud and G. Jannink, Europhys. Lett. 6 (1988) 207.
[53] L.T. Lee, O. Guiselin, A. Lapp, B. Farnoux and J. Penfold, Phys. Rev. Lett. 67 (1991) 2838.
[54] M. Daoud, B. Farnoux, G. Jannink and A. Johner, Can. J. Phys. 68 (1990) 1089.
[55] L.T. Lee, O. Guiselin, B. Farnoux and A. Lapp, Macromol. 24 (1991) 2518.
[56] A. Hariharan, S.K. Kumar and T.P. Russell, J. Chem. Phys. 98 (1993) 4163.
[57] A. Haraiharan, S.K. Kumar and T.P. Russell, J. Chem. Phys. 98 (1993) 656.
[58] R.A.L. Jones, E.J. Kramer, M.H. Rafailovich, J. Sokolov and S. Schwarz, Phys. Rev. Lett. 62 (1989) 280.
[59] G. Krausch, J. Mlynek, W. Straub, R. Brenn and J.F. Marko, Europhys. Lett. 28 (1994) 323.
[60] T.M. Slawecki, A. Karim, S.K. Kumar, T.P. Russell, S.K. Satija, C.C. Han, Y. Liu, M.H. Rafailovich, J. Sokolov and R. Overny, Europhys. Lett., submitted.
[61] S.K. Kumar, H. Tang and I. Schleifer, Mol. Phys. 81 (1994) 867.
[62] Q. Pan and R.J. Composto, Mater. Res. Soc. Symp. 366 (1995) 27.
[63] X. Zhao, W. Zhao, M.H. Rafailovich, J. Sokolov, S.K. Kumar, T.P. Russell, S.A. Schwarz and B.J. Wilkens, Europhys. Lett. 15 (1991) 725.
[64] S.A. Schwarz, B.J. Wilkens, M.A.A. Pudensi, M.H. Rafailovich, J. Sokolov, X. Zhao, W. Zhao, X. Zheng, T.P. Russell, E.J. Kramer and R.A.L. Jones, Phys. Rev. Lett. 69 (1992) 776.
[65] P. Gallagher, S.K. Satija and T.P. Russell, in preparation.
[66] A. Karim, S.K. Satija, J.F. Douglas, J.F. Ankner and L.J. Fetters, Phys. Rev. Lett. 73 (1994) 3407.
[67] S.T. Milner, Science 251 (1991) 905.
[68] S.W. Barton, W.P. Wang, D. Peiffer, M. Davis, R. Rahn and R.B. Hallock, Polym. Prep. 34 (1993) 288.
[69] D. Perahia, D.G. Wiesler, S.K. Satija, L.J. Fetters, S.K. Sinha and S.T. Milner, Phys. Rev. Lett. 72 (1994) 100.
[70] J.B. Field, C. Toprakcioglu, L. Dai, G. Hadziioannou, G. Smith and W. Hamilton, J. de Physique II 2 (1992) 2221.
[71] T. Cosgrove, P.F. Luckham, R.M. Richardson, J.R.P. Webster and A. Zarbakhsh, Coll. Surf. A 86 (1994) 103.
[72] S.M. Baker, G. Smith, R. Pynn, P. Butler, J. Hayter, W. Hamilton and L. Magid, Rev. Sci. Instr. 65 (1994) 412.
[73] G.S. Smith, C. Toprakcioglu, S.M. Baker, J.B. Field, L. Dai, G. Hadziioannou and S. Wages, Il Nuovo Cimento 16D (1994) 721.
[74] G.S. Smith, S. Wages, S.M. Baker, C. Toprakcioglu and G. Hadziioannou, Matter. Res. Soc. Symp. 376 (1994) 223.
[75] J. Penfold, E. Staples, I. Tucker and G. Fragnetto, Physica B, in press.
[76] W.A. Hamilton, P.D. Butler, S.M. Baker, G.S. Smith, J.B. Hayter, L.J. Magid and R. Pynn, Phys. Rev. Lett. 72 (1994) 2219.
[77] H.R. Brown, K. Char, V.R. Deline and P.F. Green, Macromol. 26 (1993) 4155.
[78] H.R. Brown, Macromol. 22 (1989) 2859.
[79] C.F. Creton, E.J. Kramer, C.-Y. Hui and H.R. Brown, Macromol. 25 (1992) 3075.
[80] S.H. Anastasiadis, T.P. Russell, G.P. Felcher and S.K. Satija, Macromol. 24 (1991) 1575.

[81] A. Menelle, T.P. Russell, W.A. Hamilton, G.S. Smith, S.K. Satija and C.F. Majkrzak, Macromol. 24 (1991) 5721.
[82] Y. Liu, S.A. Schwarz, W. Zhao, J. Quinn, J. Sokolov, M.H. Rafailovich, W. Dozier, L.J. Fetters and R. Dickmann, Europhys. Lett. 32 (1995) 211.
[83] D. Gersappe, D. Irvine, A.C. Balazs, Y. Liu, J. Sokolov, M.H. Rafailovich, S.Schwarz and D.G.Peiffer, Science 265 (1994) 1072.
[84] W.D. Dozier, P. Thiyagarajan, D.G. Peiffer, M. Rabeony, M.Y. Lin, G. Agrawal and R.P. Wool, Polymer 35 (1994) 3116.
[85] C. Dai, B.J. Dair, K.H. Dai, C.K. Ober, E.J. Kramer, C.-Y. Hui and L.W. Jelinski, Phys. Rev. Lett. 73 (1994) 2472.
[86] R. Kulesekere, J.F. Ankner, H. Kaiser, T.P. Russell, H.R. Brown, C. Hawker and A.M. Mayes, Macromol., submitted.
[87] E. Helfand and Z.R. Wasserman, Polym. Eng. Sci. 17 (1977) 582.
[88] G. Porod, Kolloid-Z. 124 (1951) 83.
[89] O. Glatter and O. Kratky, Small Angle X-ray Scattering (Academic Press, New York, 1982).
[90] W. Jark, G. Comelli, T.P. Russell and J. Stöhr, Thin Solid Films 170 (1989) 309.
[91] D.S. Kapp and N. Wainfan, Phys. Rev. A 138 (1965) 1490.
[92] L. Bosio, P. Keller, L. Lay-Theng, J.-P. Bourgoin and M. Vandevyver, Mol. Cryst. Liq. Cryst. 242 (1994) 71.
[93] J.J. Benattar, J. Daillant, L. Bosio and L. Leger, Colloque de Phys. C-7 (1989) 39.
[94] A. Laschewsky, H. Ringsdorf, G. Schmidt and J. Schneider, J. Am. Chem. Soc. 109 (1987) 788.
[95] I.M. Tidswell, B.M. Ocko, P.S. Pershan, S.R. Wasserman, G.M. Whitesides and J.D. Axe, Phys. Rev. B 41 (1990) 1111.
[96] F. Sun, D.W. Grainger and D.G. Castner, J. Vac. Sci. Technol. 12 (1994) 2499.
[97] Y. Lvov, G. Decher, H. Haas, H. Moehwald and A. Kalachev, Physica B 198 (1994) 89.
[98] G. Decher, Y. Lvov and J. Schmitt, Thin Solid Films 244 (1994) 772.
[99] F. Sun, G. Mao, D.W. Grainger and D.G. Castner, Thin Solid Films 242 (1994) 106.
[100] G. Krausch, Mater Sci. Eng. Rep. R14 (1995) 1.
[101] G. Krausch, E.J. Kramer, M.H. Rafailovich and J. Sokolov, Appl. Phys. Lett. 64 (1994) 2655.
[102] W. Zhao, Z. Li, M.H. Rafailovich, J. Sokolov, K. Khougav, R.B. Lennox, A. Eisenberg and G. Krausch, Nature, submitted.
[103] G. Coulon, T.P. Russell, V.R. Deline and P.F. Green, Macromol. 22 (1989) 2581.
[104] T.P. Russell, G. Coulon and D.C. Miller, Macromol. 22 (1989) 4600.
[105] S.H. Anastasiadis, T.P. Russell, S.K. Satija and C.F. Majkrzak, Phys. Rev. Lett. 62 (1989) 1852.
[106] S.H. Anastasiadis, T.P. Russell, S.K. Satija and C.F. Majkrzak, J. Chem. Phys. 92 (1990) 5677.
[107] M.D. Foster, M. Sikka, N. Singh, F.S. Bates, S.K. Satija and C.F. Majkrzak, J. Chem. Phys. 96 (1992) 8606.
[108] W.H. de Jeu, P. Lambooy, I.W. Hamley, D. Vaknon, J. Skov Pederson, K. Kjaer, R. Seyger, P. van Hutten and G. Hadziioannou, J. de Physique II 3 (1993) 139.
[109] R. Mutter, G. Strobl and B. Stühn, Fresenius' J. Anal. Chem. 346 (1993) 297.
[110] B.M. Ocko, A. Braslau, P.S. Pershan, J. Als-Nielsen and M. Deutsch, Phys. Rev. Lett. 57 (1986) 94.
[111] B.D. Swanson, H. Stragier, D.J. Tweet and L.B. Sorenson, Phys. Rev. Lett. 62 (1989) 909.
[112] P.S. Pershan and J. Als-Nielsen, Phys. Rev. Lett. 52 (1984) 759.
[113] P.S. Pershan, A. Braslau, A.H. Weiss and J. Als-Nielsen, Phys. Rev. A 35 (1987) 4800.
[114] P.S. Pershan, J. Phys. (Paris) 50 (1989) C7-1.
[115] R. Geer, S. Qadri, R. Shashidhar, A.F. Thibodeaux and R.S. Duran, Liq. Cryst. 16 (1994) 869.
[116] P. Lambooy, T.P. Russell, G.J. Kellogg, A.M. Mayes, S.K. Satija and C.F. Majkrzak, Phys. Rev. Lett. 72 (1994) 2899.
[117] A. Menelle, T.P. Russell, S.H. Anastasiadis, S.K. Satija and C.F. Majkrzak, Phys. Rev. Lett. 68 (1992) 67.
[118] N. Koneripalli, N. Singh, R. Levicky, F.S. Bates, P.D. Gallagher and S.K. Satija, Macromol. 28 (1995) 2897.
[119] P. Lambooy, T.P. Russell, G.J. Kellogg and A.M. Mayes, Phys. Rev. Lett., in press.
[120] T.P. Russell, A. Karim, A. Mansour and G.P. Felcher, Macromol. 21 (1988) 1890.
[121] A. Karim, A. Mansour, G.P. Felcher and T.P. Russell, Phys. Rev. B 42 (1990) 6846.
[122] A. Karim, A. Mansour, G.P. Felcher and T.P. Russell, Mater. Res. Soc. Symp 171 (1990) 329.
[123] G.P. Felcher, A. Karim and T.P. Russell, J. Non-Cryst. Solids 131–133 (1991) 703.
[124] A. Karim, G.P. Felcher and T.P. Russell, Macromol. 27 (1994) 6973.
[125] G. Agrawal, R.P. Wool, W.D. Dozier, G.P. Felcher, T.P. Russell and J.W. Mays, Macromol. 27 (1994) 4467, 6973.
[126] M. Stamm, S. Hüettenbach, G. Reiter and T. Springer, Europhys. Lett. 14 (1991) 451.
[127] G. Reiter and U. Steiner, J. Phys. II 1 (1991) 659.
[128] M. Stamm, D. Brautmeier, G. Reiter and M. Foster, SPE Ann. Tech. Conf. Proc. 48 (1990) 825.
[129] M. Foster, M. Stamm, G. Reiter and S. Hüttenbach, Vacuum 41 (1990) 1441.
[130] M.F. Toney, T.P. Russell, J.A. Logan, H. Kikuchi, J.M. Sands and S.K. Kumar, Nature 374 (1995) 709.
[131] W.J. Orts, J.H. van Zanten, W. Wu and S.K. Satija, Phys. Rev. Lett. 71 (1994) 867.
[132] P. Bassereau and T.P. Russell, Israel J. Chem. 35 (1995) 13.
[133] M.F. Toney and C. Thompson, J. Chem. Phys. 92 (1990) 3781.
[134] J. Daillant, J.J. Benattar, L. Bosio and L. Leger, Europhys. Lett. 6 (1988) 431.
[135] J. Daillant, J.J. Benattar and L. Leger, Phys. Rev. A 41 (1990) 1963.
[136] L. Leibler, Macromol. 20 (1987) 2535.
[137] G.H. Fredrickson and E. Helfand, J. Chem. Phys. 87 (1987) 697.
[138] F.S. Bates and G.H. Fredrickson, Ann. Rev. Phys. Chem. 41 (1990) 525.
[139] G.H. Fredrickson, Macromol. 20 (1987) 2535.
[140] M.E. Fischer, J. Vac. Sci. Technol. 10 (1973) 665.
[141] M.E. Fischer and A.N. Berker, Phys. Rev. B 26 (1982) 2507.
[142] P. Pfeuty, private communication.

[143] P. Mansky and T.P. Russell, unpublished results.
[144] A.M. Mayes, R.D. Johnson, T.P. Russell, S.D. Smith, S.K. Satija and C.F. Majkrzak, Macromol. 26 (1993) 1047.
[145] K.R. Shull, A.M. Mayes and T.P. Russell, Macromol. 26 (1993) 3929.
[146] A.M. Mayes, T.P. Russell, V.R. Deline, S.K. Satija and C.F. Majkrzak, Macromol. 27 (1994) 7447.
[147] A.M. Mayes, T.P. Russell, S.K. Satija and C.F. Majkrzak, Macromol. 25 (1992) 6523.
[148] A.M. Mayes and T.P. Russell, J. Phys. IV. Colloq. C8 (1993) 3 41.
[149] A.M. Mayes and T.P. Russell, unpublished results.
[150] P. Mansky and T.P. Russell, Macromol. 28 (1995) 8092.
[151] P. Lambooy, J.R. Salem and T.P. Russell, Thin Solid Films 252 (1994) 75.
[152] K.R. Shull, Macromol. 25 (1992) 2122.
[153] K.R. Shull, J. Chem. Phys. 94 (1991) 5723.
[154] J. Rowlinson and B. Widom, Molecular Theory of Capillarity (Oxford University Press, Oxford, 1982).
[155] D.G. Walton, G.J. Kellogg, A.M. Mayes, P. Lambooy and T.P. Russell, Macromol. 27 (1994) 6225.
[156] K.R. Shull, Macromol. 25 (1992) 2122.
[157] M. Kikuchi and K. Binder, Europhys. Lett. 21 (1993) 427.
[158] M.S. Turner, Phys. Rev. Lett. 69 (1992) 1788.
[159] K. Armundson, E. Helfand, X. Quan and S.D. Smith, Macromol. 26 (1993) 2698.
[160] K. Armundson, E. Helfand, X. Quan, S.D. Hudson and S.D. Smith, Macromol. 27 (1994) 6559.
[161] T.L. Morkved, M. Lu, A.M. Urbas, E.E. Ehrichs, H.M. Jaeger, P. Mansky and T.P. Russell, Science, submitted.